

# ENSURING HIGH YIELD AND GOOD RELIABILITY FOR MASS-PRODUCED HIGH-PERFORMANCE HALL EFFECT SENSORS

V. Mosser<sup>1</sup>, A. Kerlain<sup>1</sup>, Y. Haddab<sup>1</sup>, R. Morton<sup>2</sup>, and Martin J. Brophy<sup>2</sup>

<sup>1</sup> Itron France, 50 avenue Jean Jaurès, F-92120 Montrouge, [vincent.mosser@itron.com](mailto:vincent.mosser@itron.com), +33 146 00 6674

<sup>2</sup> TriQuint Semiconductor, 2300 NE Brookwood Pkwy, Hillsboro, OR, 97124 USA

**Keywords:** GaAs, P-HEMT, Reliability, Hall Effect, Sensor, Magnetic Sensor

## Abstract

We demonstrate the manufacturability of a very simple yet very sensitive GaAs PHEMT-based Hall sensor for home power metering applications. Initial poor Ohmic contacts were ameliorated by minimizing thermal excursions for the wafer after contacting the Ohmics. Extensive reliability testing was concluded and shows an expected failure rate of 0.01 FIT at their maximum operating temperature of 85 °C.

## INTRODUCTION

Pseudomorphic heterostructures are the basis of high performance/low cost cross-shaped Hall effect sensors that are used in the Centron® electric power meter manufactured by Itron, the best-selling power meter in the USA, with over 10 million sold. In these meters, the output of the Hall sensor directly images the consumed power. In order to achieve the rated class 0.5% meters, the allowed relative measurement error amounts to less than 0.2% in a 2000:1 dynamic range measurement. Sensors (Fig. 1) are fabricated by TriQuint on 150 mm AlGaAs/InGaAs/GaAs epi wafers from commercial epi vendors. Cost-effective manufacturing of more than four million sensors per year



**Fig. 1** A processed 150 mm wafer with over 40000 Hall sensors

faces several challenges: the specified sensor performance must be met, the yield should be kept very close to 100%, and the sensors should attain the rated lifetime of over 15 years without noticeable performance drift.

## PERFORMANCE LEVEL

The present Hall sensors have a 4-fold symmetry (Greek cross shaped) with an arm width equal to 80 µm. The Hall voltage at the output of a planar Hall sensor reads

$$V_H = r_H / en_s \cdot I_{bias} \cdot B \quad (1)$$

where in the general case the Hall scattering factor  $r_H$  depends on the sheet electron density  $n_s$ . Dealing here with a degenerate 2D channel,  $r_H$  remains equal to 1 and the cross-sensitivity of the Hall sensor reduces to  $1/en_s$ . To ensure a constant sensitivity the channel electron density  $n_s$  should meet the specified value of  $8.8 \times 10^{11} \text{ cm}^{-2}$  within a few percent, and should not drift in time by more than 0.2%. In particular, backgating-induced sensitivity drift vs. biasing current as well as temporal drift are to be avoided, as seen in Fig. 2, which shows the transient resistance change after applying a 1 mA bias current at  $t=0$ , for a good reference device and 2 defective devices with significant backgating effects. Low-bias resistance is about 3500 Ω.

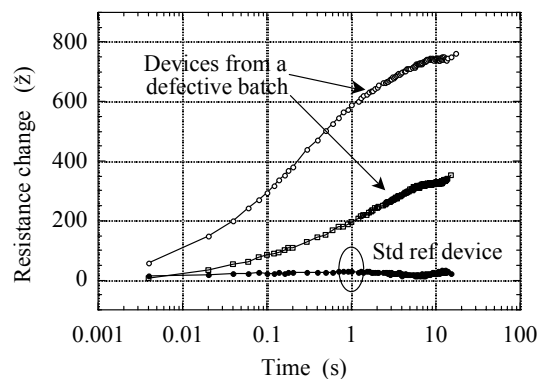


**Fig. 2** Transient resistance change after application of a 0.5 mA current step, for 2 devices from a backgating plagued batch, with a standard device as a reference.

Also, the thermal drift has to be very small and reproducible. In order to achieve these goals we developed a proprietary PHEMT-like structure, ensuring that DX centers induced by the Si doping atoms are located well above the Fermi level, and that substrate issues are well-controlled [1-4].

## YIELD ISSUES

Cost-effectiveness dictates detecting yield issues as soon as possible; therefore efficient diesort testing is

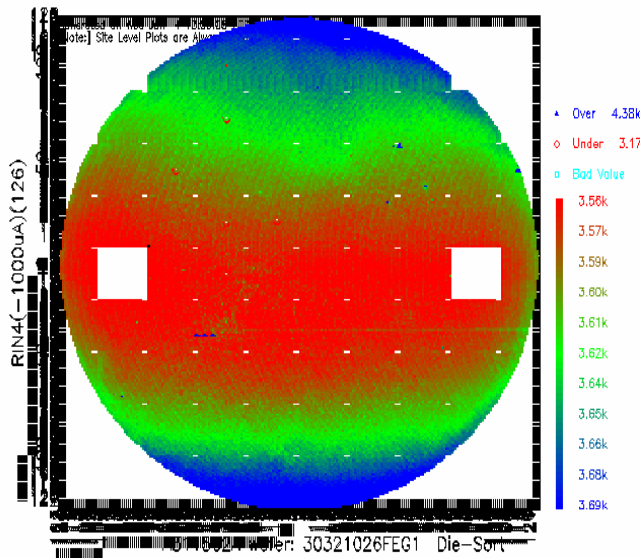


**Fig. 3 A diesort map. Center horizontal stripe = 3.56 k $\Omega$ , top and bottom dark stripes = 3.69 k $\Omega$ .**

performed at the wafer level, leading to a cartography of 40000+ positions per 6 inch wafer, as shown in Fig. 3. This map shows device resistance,  $R_{in} = 3620 \pm 60 \Omega$ .

The key parameter for the Hall-effect sensor is the electron sheet carrier concentration in the channel. It could in principle be measured using the Hall effect, however high throughput probe testing under magnetic field is not practical. Therefore, we had to devise a purely electrical characterization for checking the epi material quality and encompassing possible process-dependent performance degradation.

In particular, a standard transmission line test (TLM) was used in the Process Control Monitor to monitor the quality of the ohmic contacts. Fig. 4 shows the initial (a) and final (b) Ohmic contacts. Early in the process development the first local interconnect metal (metal 0 in TriQuint terminology) underwent a stabilizing thermal anneal. This was necessary to provide stress relief resulting in smoother morphology through subsequent processing, important when metal 0 is the bottom plate of a capacitor.

However, in this case there is no capacitor, and the annealing process was shown to only degrade the contact resistance. The process improved markedly when that customary temperature exposure not needed for this process was removed, as seen in Fig. 4b. The previously unseen degradation is related to the unique epi layer being contacted in this case, compared to implanted or epi N+ layers contacted in other processes.

## RELIABILITY ANALYSIS

### 1) Measurement procedure and results

To provide data relevant for lifetime prediction, any reliability study should first identify the most critical

degradation phenomena and which physical parameters are the most sensitive [5]. Since accurate sensors work under moderate current density and electric field strength, we had no reason to consider field or current activation, and postulated that most relevant degradation mechanisms are purely thermally activated processes.

Thus, we performed a standard accelerated aging study. Storage test were carried out at 3 different temperatures to provide an activation energy of the degradation. Based on our previous experience as well as literature, the aging temperatures were set at 250 °C, 275 °C, and 300 °C. The total duration of the aging test was 1024 hours on fifty sites. Here again, since the magnetic sensitivity cannot be conveniently measured with probe testing, we had to choose purely electrical parameters that would be exemplary of relevant degradation processes.

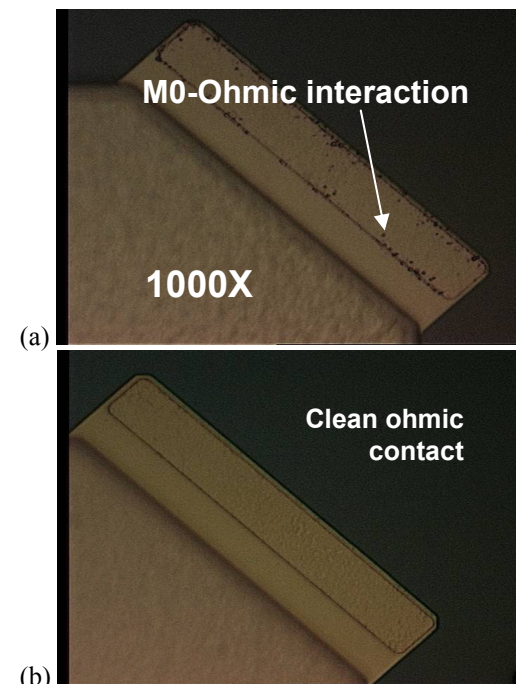
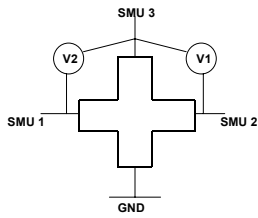


**Fig. 4 Microscope pictures of ohmic contacts (a) initial, with contact resistance  $R_c = 130 \Omega$ , and (b) optimized,  $R_c = 25 \Omega$**

Based on the experience gained in previous similar studies, we followed the behavior of the ohmic contact resistance. We added a direct measurement of the sheet resistivity  $R_{sq}$  using the van der Pauw method on the Hall sensor, in order to be able to truly separate out effects of contact resistance drift and channel resistivity drift. We also added lateral measurement of the voltage drop, in order to be able to check the behavior of the offset resistance. The procedure is illustrated in Fig. 5.

The input resistance  $R_{in}$  (as well as  $R_{in1}$ ,  $R_{in2}$ ,  $R_{L1}$  and  $R_{L2}$ ) shows a consistent behavior for all the current values, as seen for  $R_{in}$  measurements in Fig. 6a.



Quantity	Biasing current	Voltage measurement
$R_{in}$	SMU3	SMU3
$R_{in1}$	SMU1	SMU1
$R_{in2}$	SMU2	SMU2
RL1	SMU3	Voltmeter V1
RL2	SMU3	Voltmeter V2
RVDP2	SMU2	Voltmeter V2
RVDP1	SMU2	Voltmeter V1

**Fig. 5 Measurement schematics for reliability study, composed of 3 source-measure units referenced to GND and 2 differential voltmeters.**

After a 1024h thermal stress, there is a small increase (<1%) at 250°C, a still moderate increase (<2%) at 275°C, and a larger degradation (up to 15%) at 300°C. However, the sheet resistance measured by the van der Pauw method does not change, thus pointing to a degradation of the ohmic contact resistance (Fig. 6b).

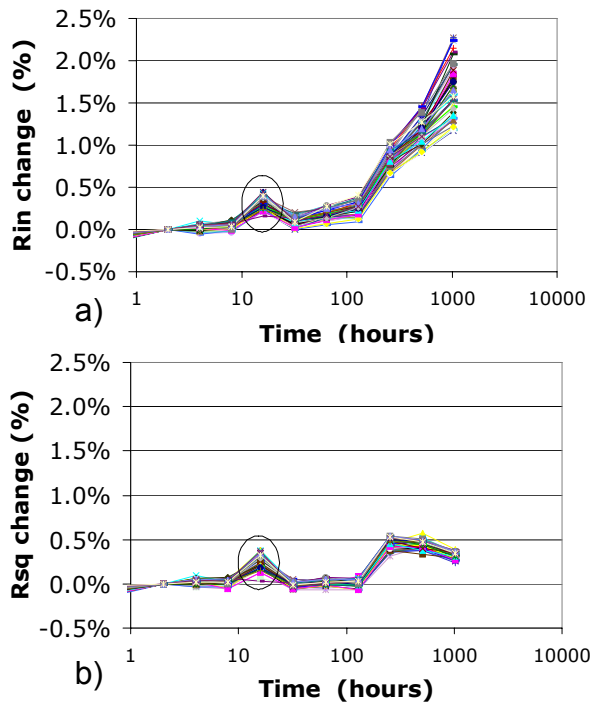


**Fig. 6 Temporal behavior (a) of the input resistance  $R_{in}$  at room temperature of a set of devices on a wafer aged at 275°C, (b) of their resistivity  $R_{sq}$ . Circled: “spike” due to the fluctuation of the measurement temperature.**

Since all relevant resistances vary with temperature with a temperature coefficient of about 0.4 %/°C, the main inaccuracy factor in this study is the ambient temperature when performing the measurements. Consequently, the temperature must be controlled tightly during the experiment to achieve the required accuracy. However, due to the small amount of resistance drift, it turns out that even with a temperature control in the  $\pm 1^\circ\text{C}$  range in the laboratory during probe testing the corresponding  $\pm 0.5\%$

resistance variation would hamper an accurate determination of the aging induced drift.

Therefore, for each location the sheet resistivity was used to monitor the wafer temperature during measurement. Indeed, based on the relationship between input resistance  $R_{in}$ , sheet resistance  $R_{sq}$  and contact resistance  $R_c$ ,

$$R_{in} = R_{sq} \cdot G + 2 R_c / W \quad (2)$$

it was verified that the normalized quantity  $R_{in}(t_i)/(G \cdot R_{sq}(t_i))$  does not show the fluctuations originating from temperature dispersion seen in  $R_{in}(t_i)$  or  $R_{sq}(t_i)$  data (Figs. 6,7). Here the geometric factor  $G$  only depends on the cross design and can be calculated e.g. by a Finite Element method. It would be equal to the aspect ratio  $L/W$  for a rectangular device. It can be easily verified that the relative drift of  $R_{in}/G \cdot R_{sq}$  can be interpreted as the ratio  $\Delta R_c(t)/R_{in}$ . That shows a linear drift vs. time, as seen in Fig. 8, denoting a slow degradation process at these very high temperatures.

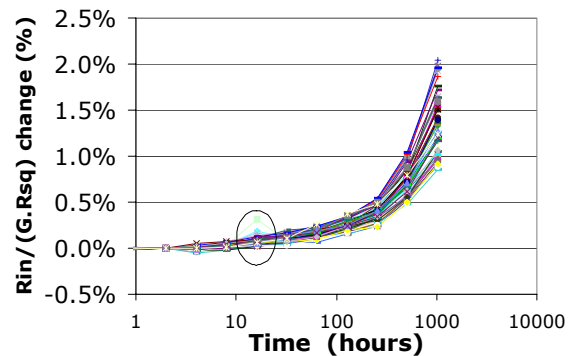


**Fig. 7 Temporal behavior (a) of the normalized quantity  $R_{in}/G \cdot R_{sq}$  at room temperature of a set of devices on a wafer aged at 275°C. Circled: temperature fluctuation “spike” cancellation due to normalization.**

For more insight into ohmic contact reliability, some TLM patterns present in PCM structures were also measured all along the accelerated aging test. The TLM study confirmed ohmic contact degradation. However, only a qualitative analysis of the PCM data could be performed, inherent to inaccurate resistance parameter extraction when using degraded TLM multi-patterns. In our case degradation analysis on Hall crosses has been found to be a much more effective, straightforward and accurate method to discriminate contact resistance degradation from the sheet resistance compared to standard contact reliability analysis based on TLM structure.

## 2) Data analysis

We first tried to perform a standard Failure Analysis based on the mortality rate for a given failure criterion at the different temperatures and assuming a lognormal distribution. However, due to the small amount of

degradation, we either saw a lot of censored data or we had to deal with a very small failure criterion  $\Delta R/R|_{fail}$ , making it difficult to extract coherent parameters. As seen in Fig. 9, the value of the activation energy found by standard Failure Analysis is largely overestimated and shows a large variation between 2 and 3.3 eV.

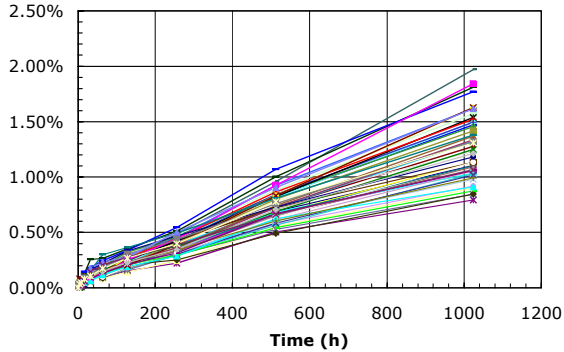


**Fig. 8 Relative drift  $\Delta R_c/R_m$  at room temperature of the contact resistance calculated from equation (1), for a set of 50 devices on a wafer aged at 275°C.**

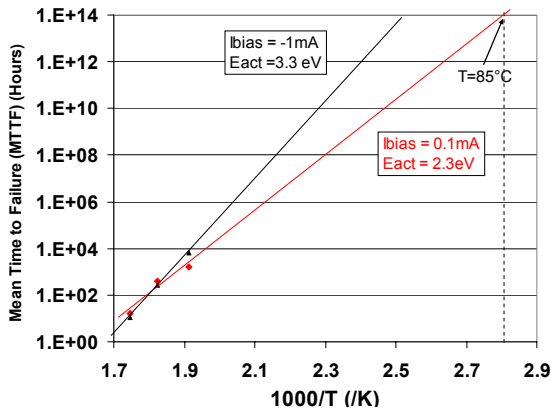


**Fig. 9 Arrhenius plot from Failure Analysis performed for tests at 250°C, 275°C, and 300°C. Depending on measurement conditions large variation of extracted activation energy are calculated.**

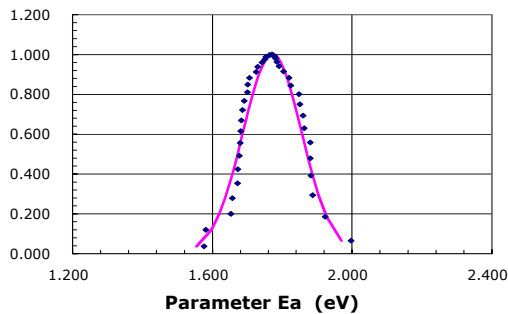


**Fig. 10 Distribution of the activation energy based on the log-normal distribution for the ohmic contact degradation from a Degradation Analysis.**

So we performed instead a Degradation Analysis based on the statistics of a thermally activated drift rate. It was found to follow a lognormal distribution. As shown in Fig. 10, Degradation Analysis provides a consistent activation energy with in the 1.7–1.8 eV range for every measurement condition. From this value, one can derive a failure rate of 1E-5 failures per year (1E-7 FIT) for an installed population of 10 million meters, if the meters were operated at room temperature, and still less than 1 failure per year (0.01 FIT) if the meter population would be permanently operated at the maximum temperature of 85°C.

## CONCLUSIONS

Mass production and application of a GaAs PHEMT Hall sensor has been successfully accomplished. High yields can be maintained without magnetic testing in production, and reliability sufficient for any normal power meter application is assured. This represents a very satisfying application of advanced compound semiconductor technology to improve performance of an important and ubiquitous appliance in every home. Moreover, it has been a commercial success, demonstrating that high tech need not be high price, high risk, nor highly unlikely for everyday applications.

## ACKNOWLEDGEMENTS

We gratefully acknowledge the work of B. Pasquier from LCIE who performed the reliability measurements.

## REFERENCES

- [1] V. Mosser, S. Contreras, S. Aboulhouda, P. Lorenzini, F. Kobbi, J.L. Robert and K. Zekentes, *Sensors&Act. A43*, 135 (1994)
- [2] V. Mosser, O. Callen, F. Kobbi, D. Adam, C. Grattapain and N. Draidia, *Materials Science and Engineering B66*, 157 (1999)
- [3] Y. Haddab, V. Mosser, F. Kobbi and R. Pond, *Microelectronics Reliability* 40, 1443-1447 (2000)
- [4] A. Kerlain and V. Mosser, *Microelectronics Reliability* 45, 1327-1330 (2005)
- [5] William J. Roesch, *Outstanding Issues in Compound Semiconductor Reliability*, Proceedings of Mantech 2005, p. 49, New Orleans, 11-14 April 2005

## ACRONYMS

- FIT: Failures in 10<sup>9</sup> hours
- P-HEMT: Pseudomorphic High Electron Mobility Transistor
- TLM: Transmission Line Method